

A traffic distribution scheme for 5G resilient backhauling using integrated satellite networks

F. Mendoza, R. Ferrús, O. Sallent
Universitat Politècnica de Catalunya (UPC)
[jesus.fabian.mendoza, ferrus, sallent]@tsc.upc.edu

Abstract – Resilience and high availability are being considered as essential requirements in 5G networks. To fulfill these requirements, the integration of a satellite component within mobile backhaul networks is regarded as a compelling proposition to provide backup connectivity to critical cell sites and divert traffic from congested areas so that a limited capacity in their terrestrial links could be supplemented during peak-time or even replaced in case of total/partial failure or maintenance. Sustained in an architectural framework that enables the integration and management of the satellite capacity as a constituent part of a SDN-based traffic engineered mobile backhaul network, this paper develops and assesses a traffic distribution strategy that exploits the dynamically steerable satellite capacity provisioned for resilience purposes to maximize a network utility function under both failure and non-failure conditions in the terrestrial links.

Keywords— *Hybrid Satellite-Terrestrial Backhaul Networks; Traffic Distribution Strategies; Resilience schemes; 5G mobile networks.*

I. INTRODUCTION

In recent years, wireless communications have taken great relevance, due to the extent of their use and the increase of critical services that are supported across multiple applications by the mobile communication networks. As pointed out in several industry papers [1][2], 5G networks are envisioned to increasingly be used as the primary means for delivering applications with high availability needs in many sectors such as critical infrastructures, manufacturing, emergency communications, automotive, health, etc. Indeed, according to [1], 5G technologies and solutions should facilitate to achieve network availability levels in the range of five nines (i.e. 99.999% of availability).

In this context, the high dependability feature attributed to satellite communications is regarded as a compelling proposition to be exploited to increase the availability and resiliency of mobile backhaul networks, complementing the terrestrial links that are commonly more susceptible to failures due to natural or man-made disasters [3]. Certainly, satellite links could provide additional bandwidth to backup connectivity to critical cell sites as well as to divert traffic from congested areas so that the capacity in the terrestrial links could be supplemented during peak-times or even replaced in case of total/partial failure or maintenance.

While the potential value of using a satellite component for resilience purposes in mobile networks is generally recognized [4][5], there is a lack of published studies aimed at assessing the benefits in terms of improved network performance that a

satellite capacity deployed for resilience purposes can bring into a hybrid terrestrial-satellite backhauling network scenario. To the best of authors' knowledge, only a few related works coping with network design and traffic engineering in hybrid satellite-terrestrial backhaul networks are available in the open scientific literature, though the applicability area is not specifically that of resilience. In particular, the works in [6]-[8] are aimed at exploiting the wide coverage capability of the satellite component for broadcast/multicast applications, showing that satellite links can relieve a Long Term Evolution (LTE) mobile network of a significant part of the multimedia broadcast multicast services traffic. Under this application, traffic distribution schemes are mainly intended to establish the best routes for multicast connections (i.e. multicast routing problem) so that the multicast performance is enhanced by seeking e.g. the minimal routing end-to-end tree delay, the minimum tree cost or other minimum failure ratio [9][10] of multicasting connections, or the combination of them [11]. Some examples of heuristic algorithms proposed in this context are given in [9][12][13]. Another addressed application area is that of emergency communications. In this context, a limited satellite capacity is typically deployed to replace terrestrial backhaul links where these are not available (e.g. terrestrial links disrupted by natural calamities) and prioritization mechanisms are applied to manage the satellite connectivity. For example, authors in [14] propose a scheme for service prioritization under traffic congestion based on the communication needs of first responders under different emergency scenarios. In a related work, [15] studies a service classification and management scheme with two traffic classes: streaming and background. The streaming traffic class gets higher priority and ensures that the constant data rate is available to the user and the rest of the satellite channel capacity is assigned to the background class and the available bit rate may vary. More recently, the issue of resilience and congestion in hybrid satellite-terrestrial wireless backhaul networks is also being researched in [16] through the implementation of smart antennas for dynamic network topology reconfiguration according to traffic demands.

Building in the utility framework model for the analysis of traffic distribution strategies and the capacity dimensioning results presented in our previous work [17], this paper develops and assesses the performance of a traffic management strategy designed to cope with a satellite capacity provisioned to improve the resilience of a hybrid satellite-terrestrial mobile backhaul network. Unlike more basic strategies that might be devised for simply replacing a failed

terrestrial link with satellite capacity or just activating traffic overflowing through satellite in high demanding peak-times, the proposed scheme pursues an optimal allocation of the available satellite and terrestrial capacity so that a network utility is maximized under both failure and non-failure terrestrial links conditions. It's worth noting that a practical implementation of such traffic distribution strategy could be achieved through the realization of the architectural framework described in [18], which enables the integration and management of the satellite capacity as a constituent part of a Software Defined Networking (SDN)- based traffic engineered mobile backhaul network in a way that end-to-end paths across the satellite and terrestrial components can be centrally computed and re-arranged dynamically at flow-level granularity in front of link congestion and failure events.

The rest of the paper is organized as follows. Section II provides the description of the system model and formulates the problem for optimal traffic distribution. Given the NP-hard nature of the resulting optimization problem, Section III describes the heuristic we've relied on for the assessment. Performance results and conclusions are then presented in Section IV and V, respectively.

II. SYSTEM MODEL AND PROBLEM FORMULATION

A. Network model

Let's consider a cellular network with M Base Stations (BS) deployed across a large geographical area. The transport connectivity between the BS and the mobile core network is assumed to be delivered through a hybrid satellite-terrestrial backhaul network. In particular, we assume that each BS site is connected to the transport infrastructure through a terrestrial link (e.g., microwave or wired link) and that there is also a Satellite Terminal (ST) co-located at each site to provide satellite connectivity. Therefore, the maximum terrestrial and satellite capacity available at BS level is represented, respectively, by the capacity vectors $\mathbf{C}^{BS} = \{C_1^{BS}, \dots, C_M^{BS}\}$ and $\mathbf{C}^{ST} = \{C_1^{ST}, \dots, C_M^{ST}\}$. In addition, it is assumed that maximum aggregate satellite capacity in use at a given time across all BS s cannot exceed C^S . Moreover, the terrestrial link availability is captured through a binary vector $\mathbf{A} = \{a_1, \dots, a_M\}$ where $a_m=1$ stands for the terrestrial link at BS_m being operational and $a_m=0$ represents a Link Down (LD) situation. An illustration of the network model is depicted in Fig 1.

B. Traffic model and utility framework

A common classification of network traffic consists of distinguishing between stream or elastic traffic. Stream traffic is generated by time-sensitive applications like Voice over IP (VoIP), Videostreaming on Demand (VSOD), etc., and typically has strict bandwidth and/or delay requirements. Elastic traffic on the other hand is generated by applications such as web browsing and file-transfers where the delivered bit rate and/or the download time are more important than inter-packet or end-to-end delays.

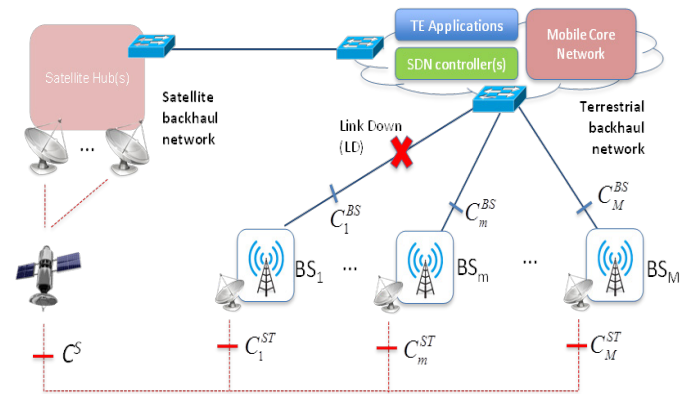


Fig. 1. Network model.

The stream/elastic traffic classification is indeed captured in the QoS model for LTE systems by considering two types of bearer services that can be enforced in the network: Guaranteed Bit Rate (GBR) bearers and Non-GBR bearers. Thus, the traffic flows served through GBR bearers (hereafter called GBR services/flows) are given a minimum guaranteed bit rate to operate satisfactorily; otherwise, the quality might be severely affected. On the other hand, the traffic flows served through Non-GBR bearers (hereafter called Non-GBR services/flows) do not get such a minimum bit rate reservation but can see a wide variability of the achieved bit rate, being more exposed to congestion related packet losses and/or delay variability (without necessarily having a noticeable impact on QoS). On this basis, the traffic demand for this study is characterised at each BS_m in terms of the number of GBR flows (ψ_m^G) and Non-GBR flows (ψ_m^{NG}). Accordingly, the total GBR and Non-GBR traffic demand across the M BS is represented as $\mathbf{T}^{GBR} = \{\psi_1^G, \dots, \psi_M^G\}$ and $\mathbf{T}^{Non-GBR} = \{\psi_1^{NG}, \dots, \psi_M^{NG}\}$ respectively.

Utility functions are then defined for GBR and Non-GBR traffic to describe the satisfaction level that is achieved when a particular flow is served with a certain bit rate. Further, the considered utility functions are defined to account for the impact on service quality due to the use of terrestrial or satellite backhaul capacity (i.e. the higher delay incurred when using a satellite link can result in some level of service degradation that is reflected with a lower utility). The utility functions under consideration are graphically depicted in Fig. 2 and explained in the following. Step functions are the ones commonly used to characterise the utility of GBR services [19]. In our case, we consider a two-level step function that reflects two possible bit rates/quality levels that could be on offer (e.g. standard and high definition VSODs). Therefore, given the delivered bit rate r and depending whether satellite ($x=0$) or terrestrial backhaul ($x=1$) is used, the utility of a GBR flow is:

$$U^{GBR}(r, x) = U_0^{GBR}(x) \cdot U_r^{GBR}(r) \quad (1)$$

where

$$U_0^{GBR}(x) = p^{GBR} + x(1 - p^{GBR}) \quad (2)$$

$$U_r^{GBR}(r) = \begin{cases} 0 & 0 < r < R_1^{GBR} \\ \alpha^{GBR} & R_1^{GBR} < r < R_2^{GBR} \\ 1 & r \geq R_2^{GBR} \end{cases} \quad (3)$$

In the previous expressions, R_1^{GBR} and R_2^{GBR} are the bit rates to be delivered for the standard and high quality offerings, respectively; the parameter $0 < p^{GBR} \leq 1$ is a utility reduction factor to account for the potential quality/satisfaction degradation when using satellite links instead of terrestrial; and the parameter α^{GBR} is a utility reduction factor to account for the impact of rate selection between R_1^{GBR} and R_2^{GBR} .

With regard to Non-GBR services, the utility functions can be more diverse [20] depending on which specific aspects/service characteristics one wants to stress. On this basis, we've adopted a logarithmic utility function [21], that is one of the most commonly used and already serves our needs. Therefore, given the delivered bit rate r and depending whether satellite ($x=0$) or terrestrial backhaul ($x=1$) is used, the utility function for a Non-GBR flow is defined as:

$$U^{Non-GBR}(r, x) = U_0^{Non-GBR}(x) \cdot U_r^{Non-GBR}(r) \quad (4)$$

where

$$U_0^{Non-GBR}(x) = p^{Non-GBR} + x(1 - p^{Non-GBR}) \quad (5)$$

$$U_r^{Non-GBR}(r) = \begin{cases} \frac{\log(r+1)}{\log(R_1^{Non-GBR}+1)} & \text{if } 0 < r < R_1^{Non-GBR} \\ 1 & \text{if } r > R_1^{Non-GBR} \end{cases} \quad (6)$$

In the previous expressions, $R_1^{Non-GBR}$ is used to establish the bit rate for which is considered that the service is already provided with a good quality (so no utility gain is envisioned by serving Non-GBR flows with higher bit rates) and the parameter $0 < p^{Non-GBR} \leq 1$ is the utility reduction factor for Non-GBR services.

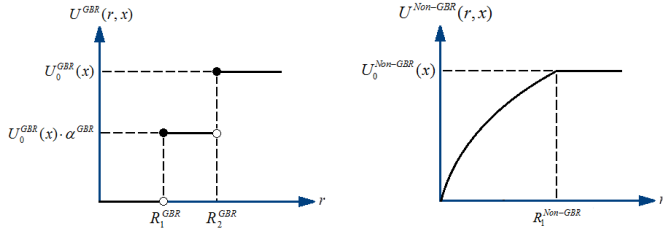


Fig. 2. Utility functions for GBR and Non-GBR services.

C. Resilience design and problem formulation for optimal traffic distribution

Different resilience schemes can be defined based on a satellite capacity allocated to cope with the failure of terrestrial links and how this capacity is intended to be used. In particular, in our case a resilience scheme is characterized by a ratio $N:M$ that indicates that the satellite capacity has been dimensioned to cope with the failure of N terrestrial links in a group of M BSs. On this basis, given the maximum transport capacity deployed at BS sites (C^{BS} and C^{ST}), the adopted resilience scheme $N:M$ (from which the maximum aggregate satellite capacity C^S is derived), the terrestrial link

availability (\mathcal{A}), and the traffic demand \mathbf{T}^{GBR} and $\mathbf{T}^{Non-GBR}$, the following optimization problem can be formulated for finding the best traffic distribution in terms of achievable bit rates and use of the terrestrial or satellite capacity per connection, represented respectively by vectors \mathbf{R} and \mathbf{X} :

Find (\mathbf{R}, \mathbf{X}) that maximizes:

$$U(\mathbf{R}; \mathbf{X}) = U^{GBR}(\mathbf{R}; \mathbf{X}) + U^{Non-GBR}(\mathbf{R}; \mathbf{X}) = \quad (7)$$

$$\sum_{m=1}^M \sum_{i=1}^{\psi_m^G} U_{m,i}^{GBR}(r_{GBR,m,i}, x_{GBR,m,i}) + \sum_{m=1}^M \sum_{j=1}^{\psi_m^{NG}} U_{m,j}^{Non-GBR}(r_{Non-GBR,m,j}, x_{Non-GBR,m,j})$$

subject to:

$$\sum_{i=1}^{\psi_m^G} r_{GBR,m,i} \cdot x_{GBR,m,i} + \sum_{j=1}^{\psi_m^{NG}} r_{Non-GBR,m,j} \cdot x_{Non-GBR,m,j} \leq a_m \cdot C_m^{BS}, \quad \forall m \quad (8)$$

$$\sum_{i=1}^{\psi_m^G} r_{GBR,m,i} \cdot (1 - x_{GBR,m,i}) + \sum_{j=1}^{\psi_m^{NG}} r_{Non-GBR,m,j} \cdot (1 - x_{Non-GBR,m,j}) \leq C_m^{ST}, \quad \forall m \quad (9)$$

$$\sum_{m=1}^M \left(\sum_{i=1}^{\psi_m^G} r_{GBR,m,i} \cdot (1 - x_{GBR,m,i}) + \sum_{j=1}^{\psi_m^{NG}} r_{Non-GBR,m,j} \cdot (1 - x_{Non-GBR,m,j}) \right) \leq C^S \quad (10)$$

$$x_{GBR,m,i}, x_{Non-GBR,m,j} \in \{0,1\}, r_{GBR,m,i}, r_{Non-GBR,m,j} \in \{0, \mathbb{R}^+\} \quad \forall m, i, j \quad (11)$$

where eq.(7) is the objective function defined as the sum of service flows utilities, eq.(8)-(10) set out, respectively, the capacity constraints of terrestrial links per BS, satellite links per BS and maximum aggregated satellite capacity and eq.(11) restricts the possible values of the decision variables. The resulting problem is a non-linear optimization problem that falls within the category of non-convex mixed-integer nonlinear programming, which is known to be NP-hard [22].

III. TRAFFIC DISTRIBUTION STRATEGY ALGORITHM

Given the NP-hard nature of the optimization problem formulated in section II.C, we've developed an heuristic algorithm that can handle, with low complexity, large scenarios in terms of number of BSs and traffic flows. The proposed algorithm seeks to find a feasible solution to the optimization problem by splitting it into two separate sub-problems:

- First, the bit rate allocation and path selection through either terrestrial or satellite backhaul is computed for the GBR connections. This is done on a connection-basis trying to allocate, per BS and sequentially, the link and bit rate that provides the highest utility per connection. When capacity constraints are reached, the algorithm attempts to allocate pending connections by gradually reducing the utility of the new as well as of the pre-established connections as long as the global utility (i.e. term $U^{GBR}(\mathbf{R}; \mathbf{X})$ in Eq. 7) can be still increased. The procedure is detailed Table I, algorithm 1.
- Second, the remaining satellite capacity is distributed seeking a max-min rate allocation for Non-GBR connections irrespective of using satellite or terrestrial capacity. It's worth noting that a max-min rate allocation is equivalent to the maximization of the global utility of Non-GBR traffic (i.e. term $U^{Non-GBR}(\mathbf{R}; \mathbf{X})$ in Eq. 7) when there is no distinction between using satellite or terrestrial

capacity [23], which in our case is strictly valid for factor $p^{Non-GBR}=1$. This is carried out by first distributing the satellite capacity among the *BSs* in proportion to the number of GBR connections handled per *BS* so that overall capacity left for GBR services is balanced across *BSs*. Then, in each *BS*, the satellite capacity is equally shared among the served connections. The detailed procedure is given as algorithm 2 in Table I.

TABLE I. TRAFFIC DISTRIBUTION ALGORITHMS

Algorithm 1: Resource allocation for GBR connections	
Procedure "Find (R,X) for GBR connections"	
1.	$T_m^G \leftarrow 0, S_m^G \leftarrow 0, \varphi_m^G \leftarrow \psi_m^G, CR_m^{BS} \leftarrow C_m^{BS} \quad \forall m$
2.	for $m=1..M$ do
3.	if ($C_m^{BS} \geq \psi_m^G \cdot R_2$) then
4.	$x_{GBR,m,i} \leftarrow 1, r_{GBR,m,i} \leftarrow R_2, \varphi_m^G \leftarrow 0, T_m^G \leftarrow \psi_m^G, \forall i$
5.	else
6.	if ($U^{GBR}(R_2, I) + U^{GBR}(R_2, 0) < 2U^{GBR}(R_1, I)$) then
7.	$x_{GBR,m,i}, r_{GBR,m,i} \leftarrow \arg \max U(I, r_{GBR,m,i}) \forall i: i \in \varphi_m^G, \varphi_m^G \leftarrow \varphi_m^G - T_m^G, \text{ s.t. eq.(8)}$
8.	if ($\varphi_m^G > 0$) then
9.	$x_{GBR,m,i}, r_{GBR,m,i} \leftarrow \arg \max U(0, r_{GBR,m,i}) \forall i: i \in \varphi_m^G, \varphi_m^G \leftarrow \varphi_m^G - S_m^G, \text{ s.t. eq.(9-10)}$
10.	$x_{GBR,m,i} \leftarrow 1, r_{GBR,m,i} \leftarrow 0, \forall i: i \in \varphi_m^G$
11.	end if
12.	else if
13.	for $i \in \varphi_m^G$ do
14.	$x_{GBR,m,i} \leftarrow 1, r_{GBR,m,i} \leftarrow R_2, T_m^G \leftarrow T_m^G + 1, \varphi_m^G \leftarrow \varphi_m^G - 1, \text{ s.t. eq.(8)}$
15.	if eq.(8) constraint is not satisfied then
16.	$x_{GBR,m,i} \leftarrow 0, r_{GBR,m,i} \leftarrow R_2, S_m^G \leftarrow S_m^G + 1, \varphi_m^G \leftarrow \varphi_m^G - 1 \text{ s.t. eq.(9-10)}$
17.	if eq.(9-10) constraints are not satisfied then goto step 20;
18.	end if
19.	end for
20.	for $i \in \varphi_m^G$ do
21.	rate reduction of T_m^G connections: $x_{GBR,m,i} \leftarrow 1, r_{GBR,m,i} \leftarrow R_1$ and U_m^{GBR} is increased. $T_m^G \leftarrow T_m^G + 1, \varphi_m^G \leftarrow \varphi_m^G - 1, \text{ s.t. eq.(8)}$
22.	if eq.(8) constraint is not satisfied then
23.	rate reduction of S_m^G connections: $x_{GBR,m,i} \leftarrow 0, r_{GBR,m,i} \leftarrow R_1$ and U_m^{GBR} is increased. $S_m^G \leftarrow S_m^G + 1, \varphi_m^G \leftarrow \varphi_m^G - 1, \text{ s.t. eq.(9-10)}$
24.	if eq.(9-10) constraints are not satisfied then
25.	for $i \in \varphi_m^G$ do
26.	$x_{GBR,m,i} \leftarrow 1, r_{GBR,m,i} \leftarrow 0, \varphi_m^G \leftarrow \varphi_m^G - 1$
27.	end for
28.	end if
29.	end if
30.	end for
31.	end else if
32.	end else if
33.	end for
34.	end procedure
Algorithm 2: Resource allocation for Non-GBR connections	
Procedure "Find (R,X) for Non-GBR connections"	
1.	$CR_m^{BS} \leftarrow$ remaining terrestrial capacity after GBR allocation
2.	$CR_m^S \leftarrow$ remaining satellite capacity after GBR allocation
3.	$val_m \leftarrow CR_m^{BS} / \psi_m^{NG}, \forall m$
4.	$val_{max} \leftarrow \arg \max (val_m), \text{ s.t. } (\sum_m (val_{max} - val_m) \cdot (\psi_m^{NG})) \leq CR_m^S, \forall m: val_m < val_{max}$
5.	$C_m^{ST} \leftarrow (val_{max} - val_m) \cdot (\psi_m^{NG}), \forall m: val_m < val_{max}$
6.	$C_m^{ST} \leftarrow 0, \forall m: val_m \geq val_{max}$
7.	$S_m^{NG}, T_m^{NG} \leftarrow \text{solve } (C_m^{ST} / S_m^{NG} \sim CR_m^{BS} / T_m^{NG}), \forall m: val_m < val_{max}$
8.	$S_m^{NG} \leftarrow 0, T_m^{NG} \leftarrow \psi_m^{NG}, \forall m: val_m \geq val_{max}$
9.	$C_m^{ST} \leftarrow (S_m^{NG} / \sum_{m=1}^M S_m^{NG}) \cdot CR_m^S, \forall m: val_m < val_{max}$
10.	for $m=1..M$ do
11.	while $U^{Non-GBR}(R; X)$ increases do
12.	$S_m^{NG} \leftarrow S_m^{NG} - 1, T_m^{NG} \leftarrow T_m^{NG} + 1$
13.	$x_{Non-GBR,m,j} \leftarrow 0, r_{Non-GBR,m,j} \leftarrow C_m^{ST} / S_m^{NG} \quad \forall j \in S_m^{NG}$
14.	$x_{Non-GBR,m,j} \leftarrow 1, r_{Non-GBR,m,j} \leftarrow CR_m^{BS} / T_m^{NG}, \forall j \in T_m^{NG}$
15.	end while
16.	end for
17.	end procedure
Notation:	
T_m^G :	Terrestrial GBR connections at BS_m
T_m^{NG} :	Terrestrial Non-GBR connections at BS_m
S_m^G :	Satellite GBR connections at BS_m
S_m^{NG} :	Satellite Non-GBR connections at BS_m
φ_m^G :	Non-processed GBR connections at BS_m
CR_m^{BS} :	Non-utilized terrestrial capacity at BS_m
val_m :	Non-GBR rate considering only terrestrial resources at BS_m

IV. NUMERICAL ASSESSMENT

A. Simulation method and scenario Settings

The numerical assessment is based on a Monte Carlo simulation method that solves the traffic distribution problem in a set of 1000 realizations. In each realization, a random number of GBR and Non-GBR connections is generated per *BS* according to a uniform distribution. Table II provides the range of values considered for the different model parameters in the numerical assessment. With regard to the capacity of the terrestrial links, the considered setting (131 Mbps) is based on the dimensioning analysis presented in [17] to cope with the 90-th percentile of the traffic demand when considering a realistic traffic model that exhibits a log-normal distribution with an average load of 100 Mb/s per *BS*. This value is then considered to establish the range of values for the maximum aggregate satellite capacity (C^S) according to the adopted resilience scheme. On the other hand, the maximum satellite link capacity per *BS* (C^{ST}) is set to 200 Mb/s, in line with today's top-of-the-line satellite modems based on DVB-S2X [24].

TABLE II. SCENARIO SETTINGS FOR THE NUMERICAL ASSESSMENT

Parameter	Range of values
Number of <i>BS</i> (M)	16
Terrestrial link capacity (C^{BS})	131 Mbps at each <i>BS</i>
Terrestrial link availability (A)	0-4 links down
Maximum satellite link capacity per <i>BS</i> (C^{ST})	200 Mbps at each <i>BS</i>
Resilience scheme	NR, 1:16, 1:8, 1:4
Maximum aggregate satellite capacity (C^S)	0, 131, 262, 524 Mbps
Average number of GBR Connections per <i>BS</i>	0-50
Average number of Non-GBR conn. per <i>BS</i>	0-50
Standard quality rate for GBR conn. (R_1^{GBR})	3 Mbps*
High quality rate for GBR connections (R_2^{GBR})	6 Mbps*
Utility reduction factor due to GBR rate sel. (a^{GBR})	0.6
Maximum utility rate Non-GBR conn. ($R_1^{Non-GBR}$)	13 Mbps**
Utility reduction factor over sat. (p^{GBR} and $p^{Non-GBR}$)	0.6, 0.8, 1

* Typical mobile Video Resolution and Bitrates [25]

** The global average for LTE download speed [26]

B. Assessment under no Link Failure Conditions

This first assessment is intended to show the performance of the traffic distribution strategy when all terrestrial links are operational (i.e. LD=0). Unlike a more classical approach where the satellite capacity is only used as failover/back-up, the idea here is to see how the proposed strategy can get the most utility out of all the installed capacity.

Focusing first on the GBR traffic performance, the achieved average utility per GBR connection when no satellite capacity for resilience is deployed (NR case) is given in Fig. 3, along with the utility gain achieved when considering the different resilience schemes (RS1:16, RS1:8 and RS1:4) under different GBR traffic loads. It is observed that, under NR, up to around 15 GBR connections can be served on average per *BS* while achieving the maximum utility. From that point, utility starts to decrease and it's when the satellite capacity gets into play to deliver the amount of utility gain depicted on the figures on the right-hand axis. In particular, achieved utility gains for RS=1:4 sit between 8% (considering a factor $p^{GBR}=0.6$) and 18% (considering a factor $p^{GBR}=1$) when the number of connections goes between 25-30, therefore raising

the utility achieved from 80% under NR to levels between 88% and 98% under RS=1:4. Similar trends are obtained for Non-GBR traffic, as illustrated in Fig. 4, noting however that in this case the utility increase can even reach higher values.

The impact on the allocated bit rates is depicted in Fig. 5. For GBR connections, the availability of satellite capacity makes that average number of GBR connections per *BS* that can be served at full rate increases from 15 to 26 connections (70% increase) for RS1:4. For Non-GBR connections, Fig. 5(b) depicts the CDF of the bit rates allocated to Non-GBR traffic under different Non-GBR loads (5,15 and 25) and considering 5 GBR connections per *BS* and $p^{Non-GBR}=0.8$. It can be seen as the use of a resilience scheme with higher satellite capacity does not only achieves the highest rates but also allows for a more equitable bit rate distribution among the network connections, reducing the gap of rates assigned among the Non-GBR connections. For example, if we get the Non-GBR rates within the percentiles 10% - 90%, for 15 Non-GBR connections, we get a gap of only 2 Mbps for RS1:4, while we get the gap of 3.7 Mbps and 4.5 Mbps for RS1:16 and NR respectively, this is, a reduction of almost 50% of the gap of rates when is used the resilience scheme with greatest capacity. This is due to the satellite capacity is distributed dynamically in proportion to the load on each *BS*, thus maintaining equitably the data rates allocated among all connections.

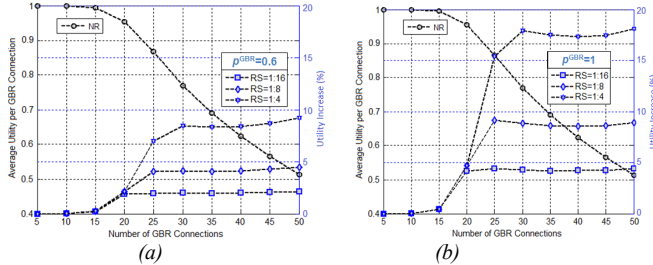


Fig. 3. Average Utility per GBR connection and Utility Increase.

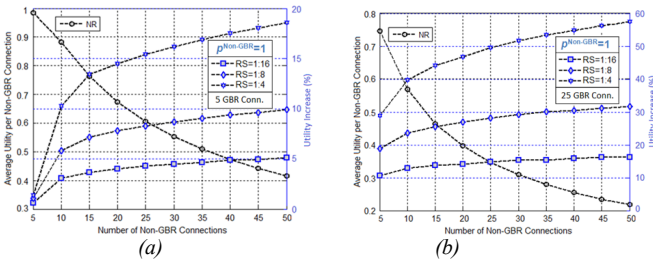


Fig. 4. Average Utility per Non-GBR connection and Utility Increase for two GBR loads: (a) 5 and (b) 25 GBR connections per *BS*.

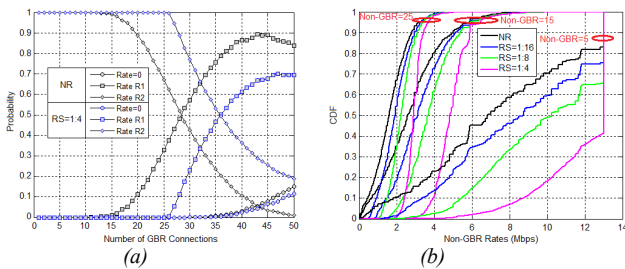


Fig. 5. a) PDFs of GBR bit rates for NR and RS=1:4. b) CDF of bit rates assigned to Non-GBR connections.

C. Assessment under Link Failure Conditions

Fig. 6 (a) provides the average utility decrease per GBR connection achieved in the *BS*s that are affected by terrestrial link failures ($LD=2$) in comparison with the case without link failures. Under low load conditions, it can be observed that the minimum utility decrease is lower bounded by the value of p^{GBR} , meaning that all the traffic served by the impaired *BS*s can be successfully diverted through the satellite capacity. This utility decrease can be kept at this minimum value up to an average of 10 connections per *BS* when considering the resilience scheme with smaller satellite capacity ($RS=1:16$) and up to 24 connections for the resilience scheme with higher capacity ($RS=1:4$). Therefore, while the utility decrease would be of 100% for the NR case (i.e. no traffic can be served through the affected *BS*), the use of the satellite capacity can keep the utility reduction to values below 30% (i.e. overall utility for GBR traffic above 70%) for a traffic load ranging from 20 to 30 GBR connections per *BS*. For Non-GBR traffic, Fig. 6 (b) shows that the impact in utility reduction is higher than that experienced by GBR connections due to preferential treatment given by the traffic distribution algorithm. Moreover, additional results not included in the presented figures, show that there is also some utility reduction in the *BS* not directly affected by the terrestrial link failures, even though this reduction is below 4% for GBR and Non-GBR connections compared to the case that all links were up.

Finally, Fig. 7 presents the impact of the link failures in terms of the allocated bit rate distribution. For GBR traffic, the average number of GBR connections that can be still served at full rate increases from 7 to 23 (200% increase) when comparing RS1:4 and RS1:16, as depicted in Fig. 7 (a). Likewise, the average number of GBR connections per *BS*, supported with at least the minimum rate R_1 , is above 100% higher for RS1:4 than for RS1:16 (from 10 to 22 connections on average per *BS*). With regard to Non-GBR bit rates, Fig. 8 (b) provides the CDF of the allocated bit rates for $LD=2$ and RS1:16, 1:8 and 1:4, showing the relative performance of these schemes against the a worst performing case ($LD=2$ and NR) and a best performing case ($LD=0$ and RS1:4).

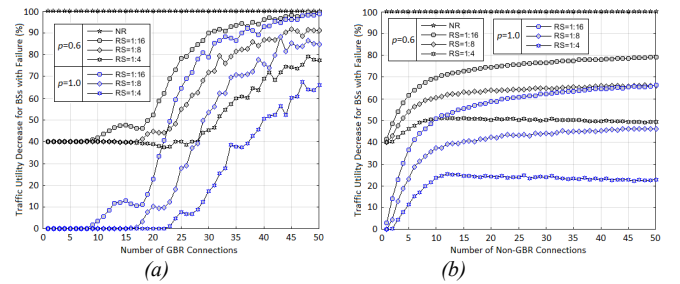


Fig. 6. Average utility reduction in *BS*s affected by link failures. a) GBR connections. b) Non-GBR connections.

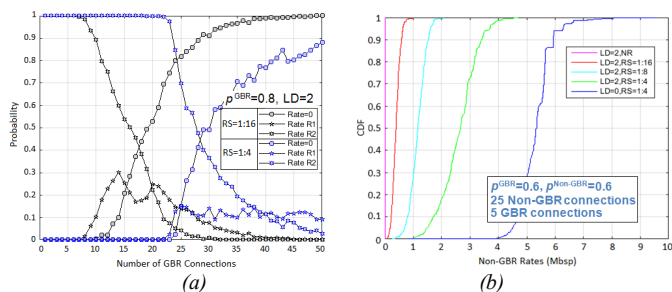


Fig. 7. a) PDFs of GBR bit rates for RS=1:16 and RS=1:4. b) CDF of bit rates assigned to Non-GBR connections.

V. CONCLUSIONS

The integration of a satellite component within mobile backhaul networks is regarded as a compelling proposition to increase its availability and resiliency.

This paper has developed and numerically assessed by means of simulation a traffic distribution strategy that exploits a dynamically steerable satellite capacity provisioned for resilience purposes to maximize a network utility function. The analysis has considered different resilience schemes, characterized by the ratio $N:M$ of satellite capacity needed to cope with the failure of N terrestrial links in a group of M BSs. Obtained results show how, under failure conditions, the proposed traffic distribution strategy is able to redistribute the satellite resources so that the utility decrease in the BSs affected by terrestrial link failures is minimized. And remarkably, when all the terrestrial links are fully operational, it's been shown that the proposed strategy does not leave the satellite capacity unused but exploits it in order to improve the overall network utility.

The presented results give us some fundamental guidelines for deriving design and dimensioning principles to consider resilience as a built-in feature in 5G systems. Future work considers a deeper analysis of the optimality conditions and algorithms to cope with the presented optimization problem as well as its extension to jointly consider other uses of the 5G backhaul integrated satellite capacity such as fast deployments/special events and the delivery of multicast traffic.

ACKNOWLEDGMENT

Research leading to these results has received funding from the European Union's H2020 Research and Innovation Programme (H2020-ICT-2014-1) under the Grant Agreement H2020-ICT-644843 and by the Spanish Research Council and FEDER funds under RAMSES grant (ref. TEC2013-41698-R).

REFERENCES

- [1] NGMN Alliance, "5G White Paper", February 2015
- [2] Sacchi, Osseiran A., Boccardi F., Braun V., Kusume K., Marsch P., Maternia M., Queseth O., Schellmann M., Schotten H., Taoka H., Tullberg H., Mikko A. Uusitalo, Timus B., and Fallgren M., "Scenarios for 5G Mobile and Wireless Communications: The Vision of the METIS Project", IEEE Communications Magazine, May 2014.
- [3] Sacchi C., Bhasin K., Kadowaki N., Vong F., "Toward the SPACE 2.0 era", IEEE Communications Magazine, pp. 16-17., March 2015.

- [4] NetWorld2020's – SatCom WG The role of satellites in 5G, Version 5 – 31th July 2014
- [5] Watts S., Glenn O., "5G resilient backhauling using integrated satellite networks", IEEE Advanced Satellite Multimedia System Conference, September 2014.
- [6] N. Cassiau and D. Ktenas, "Satellite Multicast for Relieving Terrestrial eMBMS: System-Level Study," 2015 IEEE 82nd Vehicular Technology Conference (VTC2015-Fall), Boston, MA, 2015, pp. 1-5.
- [7] E. H. K. Wu and Chao-hsu Chang, "Adaptive multicast routing for satellite-terrestrial network," Global Telecomm. Conference, 2001. GLOBECOM '01. IEEE, San Antonio, TX, 2001, pp. 1440-1444 vol.3.
- [8] N. Chuberre1, O. Courseille1, P. Laine2, L. Rouillet2, T. Quignon1 and M. Tatard, "Hybrid satellite and terrestrial infrastructure for mobile broadcast services delivery: An outlook to the 'Unlimited Mobile TV' system performance", International journal of satellite communications int. J. Commun. Syst. Network 2008; 26: 405-426 Published online in Wiley InterScience(www.interscience.wiley.com).DOI: 10.1002/sat.910.
- [9] E. H. K. Wu and Chao-hsu Chang, "Adaptive multicast routing for satellite-terrestrial network", IEEE Global Telecommunications Conference, 2001 (GLOBECOM '01), San Antonio, TX, 2001
- [10] Laxman H. Sahasrabudde and Biswanath Mukherjee, "Multicast Routing Algorithms and Protocols: A Tutorial", IEEE Net., Jan 2000.
- [11] Zhizhong Yin, Long Zhang, Xianwei Zhou, Peng Xu, Yu Deng, "QoS-Guaranteed Secure Multicast Routing Protocol for Satellite IP Networks Using Hierarchical Architecture", Int. J. Communications, Network and System Sciences, 2010
- [12] Eylem E., Ian F. Akyildiz, and Bender M., "A Multicast Routing Algorithm for LEO Satellite IP Networks", IEEE/ACM TRANSACTIONS ON NETWORKING, VOL. 10, n° 2, April 2002
- [13] De-Nian Yang, Wanjiun Liao, "On multicast routing using rectilinear Steiner trees for LEO satellite networks", IEEE Comm. Society, Globecom 2004
- [14] C. A. Grazia et al., "Integration between terrestrial and satellite networks: the PPDR-TC vision," 2014 IEEE 10th International Conference on Wireless and Mobile Computing, Networking and Communications (WiMob), Larnaca, 2014
- [15] E. H. Fazli, M. Werner, N. Courville, M. Berlioli and V. Boussemart, "Integrated GSM/WiFi Backhauling over Satellite: Flexible Solution for Emergency Communications", Vehicular Technology Conference, 2008. VTC Spring 2008. IEEE, Singapore, 2008
- [16] SANSa (Shared Access Terrestrial-Satellite Backhaul Network enabled by Smart Antennas) research project, HORIZON 2020 Framework Programme. Website: <http://www.sansa-h2020.eu/>
- [17] Mendoza F., Ferrús R., Sallent O., "Flexible Capacity and Traffic Management for Hybrid Satellite-Terrestrial Mobile Backhauling Networks", 2016.
- [18] R. Ferrus, O. Sallent, T. Ahmed, R. Fedrizzi, "Towards SDN/NFV-enabled satellite ground segment systems: End-to-End Traffic Engineering Use Case", accepted for publication in ICC'17 1st International Workshop on Satellite Communications - Challenges and Integration in the 5G ecosystem, Paris, 21-25 May 2017.
- [19] S. Shenker, "Fundamental Design Issues for the Future Internet", IEEE J-SAC, vol.13, no.7, pp.1176-1188, Sep.1995.
- [20] Zhimei Jiang, Ye Ge, Ye Li, "Max-utility wireless resource management for best-effort traffic", IEEE Trans. Wireless Comm, vol.4, no.4, pp.100-111, Jan.2005.
- [21] E. Kelly, "Charging and rate control for elastic traffic," European Trans.Telecomm, vol.8, pp.33-37, 1997.
- [22] S. Burera, A. N. Letchfordb, "Non-convex mixed-integer nonlinear programming: A survey", Surveys in Operations Research and Management Science, Volume 17, Issue 2, July 2012, Pages 97-106.
- [23] T. Harks, "Utility Proportional Fair Bandwidth Allocation: An Optimization Oriented Approach," in QoS-IP, pp. 61-74, 2005.
- [24] ESA news: <https://artes.esa.int/news/newtec-introduces-industrys-first-dvb-s2x-vsatsat-modem>. Last access on 18 November 2016
- [25] "Video as a Basic Service of LTE Networks: Mobile vMOS Defining Network Requirements". Huawei. 2015. <http://www.huawei.com/minisite/4-5g/en/industryjsdc-j.html>
- [26] OpenSignal. "The State of LTE" February 2016. <http://opensignal.com/reports/2016/02/state-of-lte-q4-2015/>